Progress In Electromagnetics Research M, Vol. 75, 21–28, 2018

FDTD Based Dictionary Matrix for Sparsity-Based Through-Wall Radar Imaging

Fang-Fang Wang[1, 2, *], Sichao Zhong[3], Huiying Wu[2], Tingting Qin[2], and Wei Hong[1]

Abstract—Compressive sensing for through-wall radar imaging (TWRI) is a promising method to obtain a high-resolution image with limited number of measurements. The capability of the existing method in the framework of CS is limited due to the model error stemmed from the approximated signal model which does not consider multipath returns or only consider first-order interior wall multipath returns. In order to exploit various multipath returns, finite-difference time domain (FDTD) technique is used to obtain the scattered signal for each assumed target position and then to construct the exact forward scattering model. Then, sparse reconstruction is used to solve this linear inverse problem. Numerical results demonstrate that the proposed approach performs better at ghost suppression in the same condition of the signal-to-noise ratio (SNR).

1. INTRODUCTION

Sensing through obstacles, such as walls, doors, and other visually opaque materials using microwave signals, is emerging as a powerful tool which supports a range of civilian and military applications [1]. Through-wall radar imaging (TWRI) is an emerging technology that allows non-invasive surveys of the region of interest behind the front wall by providing high-resolution images [2, 3].

New and innovative approaches have been continuously proposed over the last decades. However, as a new radar imaging technology applied in complex environments, TWRI still has many challenges. High-resolution imaging demands large bandwidth signal and large array aperture which lead to large amounts of data. Thus one remaining challenge for TWRI development is that how to alleviate processing bottleneck of high-speed data acquisition, storing, and transmission [4].

The new emerging theory of compressive sensing (CS) provides an idea to reduce the cost of data acquisition. CS states that it is possible to accurately recover an unknown sparse signal from a limited number of measurements with high probability by solving a convex optimization problem [5, 6]. Making use of the sparsity of the scene, CS was widely applied in TWRI, providing an efficient way of image reconstruction using far fewer observations [7–10].

Another major challenge in TWRI is the presence of multipath signals originating from the interaction of the target with the surrounding structures. When multipath is not correctly accounted in the model, false targets or "ghosts" will be introduced in the image. Therefore, the imaged scene becomes highly cluttered and difficult or even impossible to be interpreted [11].

Existing methods have addressed the issue of multipath propagation in through-wall (TW) scenarios [12, 13]. Earlier works assumed that multipath propagation is a nuisance. Therefore, some approaches were proposed to effectively mitigate the effects of it. More recent works are based on the multipath exploitation. In particular, an analytical model which takes into account

Received 22 August 2018, Accepted 4 October 2018, Scheduled 18 October 2018
* Corresponding author: Fangfang Wang (wangff@njupt.edu.cn).
[1] State Key Laboratory of Millimeter Waves, Southeast University, Nanjing 211189, China. [2] School of Electronic Science and Engineering, Nanjing University of Posts and Telecommunications, Nanjing 210003, China. [3] Jiangsu Branch of National Computer Network Emergency Response Technical Team/Coordination Center of China, Nanjing 210003, China.

multipath propagations for TWRI scenario has been presented by Setlur et al. with the aim to locate multipath ghosts and associate them with the true target position, thus improving the signal-to-clutter ratio [14, 15].

Motivated by the idea of multipath exploitation and compressive sensing, Leigsnering et al. combine the two methods to achieve good image reconstruction in multipath environments from far fewer spatial and frequency measurements [16–18]. Specifically, their approach calculates some multipath propagation paths for each assumed target position with the geometric optics (GO) or ray-tracing approach which is established based on the fact that electromagnetic waves propagate as optical rays, which are governed by Snell's laws. Therefore, a forward scattering model is developed for multipath to be properly exploited in the framework of sparse recovery.

Since TWRI problem involves a noncanonical geometry, multipath returns for it can be categorized to interior wall multipath, wall ringing multipath and target-to-target interaction. Furthermore, the interior wall multipath returns are divided into first-order multipath and higher-order multipath. Actually, the various multipath returns are very hard to be calculated using GO considerations. In addition, the number of multipath returns is hard to be determined even if the building layout is known a priori. Leigsnering's works only compute the first-order interior wall multipath returns, while other multipath returns are neglected. Therefore, no exact signal model is ready up to now.

Finite-difference time domain (FDTD) is the most popular numerical technique for solving complex electromagnetic problems [19]. Different from GO approach, the background medium can be described by the Green's function that depicts the impulse response of the wave equation in the FDTD simulation. Moreover, it is quick to code the FDTD method for a specific problem and gain the forward scattering electromagnetic fields. In this paper, a series of FDTD numerical simulations are applied to calculate the exact signal model which contains all kinds of multipath returns. Specifically, for each assumed target position, an FDTD simulation is performed to obtain the corresponding scattering signals at each receiving antenna position and then stack them into a column. All of these columns form the dictionary matrix of the linear signal model. It is noted that all kinds of multipath returns in through wall scenario can be calculated simultaneously using FDTD simulation. FDTD allows developing correct forward model and CS allows reducing data, thus the combination of them can solve the two major challenges simultaneously and be able to obtain a ghost-free image with less data processing burden.

This paper is organized as follows. Section 2 presents the signal model incorporating various multipath returns calculated based on FDTD. A CS framework is used to solve the linear model in Section 3. Section 4 presents some simulation results, and conclusion follows in Section 5.

2. SIGNAL MODEL

2.1. Basic Signal Model

Bistatic synthetic aperture radar (SAR) system is used in this paper. Suppose that a UWB impulse radar system with one transmitter placed near the wall interrogates the scene by transmitting wideband Gaussian pulse $s(t)$. A receiver is mounted on a vehicle moving parallel to the wall to synthesize an N-element aperture and receives signal consisting of M time samples at each position. Under this operation, the mth time sample of P targets return received at the nth synthetic aperture location can be expressed as

$$y(m,n) = \sum_{p=0}^{P-1} \sigma_p s(t_m - \tau_{np}) \tag{1}$$

Here σ_p is the reflectivity of the target, which is assumed to be independent of frequency and aspect angle, and τ_{np} is the round-trip propagation delay of the signal from the transmitter to the pth target and then to the nth receiver location.

The target space behind the wall is partitioned into rectangular grids, with K pixels along the cross range and L pixels along the downrange. Then the target return is given by

$$y(m,n) = \sum_{k,l=1}^{K,L} \sigma_{k,l} s(t_m - \tau_{n,(k,l)}) \tag{2}$$

$\sigma_{(k,l)} = \sigma_p$ if a target exists at the $(k, l)th$ pixel; otherwise, $\sigma_{(k,l)} = 0$. All MN measurements $y(m, n)$ are stacked into a single column to obtain the measurement data vector.

$$y = [y(1,1), \ldots, y(M,1), \ldots y(M,N)]^T \tag{3}$$

As such, Eq. (2) can be formally expressed as

$$\mathbf{y} = \mathbf{\Phi x} \tag{4}$$

In Eq. (4), $\mathbf{\Phi}$ is the $MN \times KL$ matrix that relates the unknown vector to the data vector, and it represents the dictionary under the framework of sparse representation. The (i, j)th element of $\mathbf{\Phi}$ is given by

$$[\mathbf{\Phi}]_{ij} = s(t_m - \tau_{n,(k,l)}) \tag{5}$$

for $m = \lceil i/M \rceil$, $n = \lfloor i/M \rfloor$, $k = \lceil j/K \rceil$, and $l = \lfloor j/K \rfloor$. $x = [\sigma_{1,1}, \ldots \sigma_{K,L}]^T$ is the scene reflectivity vector.

2.2. Multipath Propagation Model

In TWRI, the target can be hidden behind layered or inhomogeneous cinder block walls or inside an enclosed room. As a consequence, multipath stemming from multiple reflections of electromagnetic waves from the target to the walls, floors, and ceiling will cause "ghost targets" if it is not correctly mitigated or exploited. Considering one direct path and $R-1$ first-order interior wall multipath returns for each target-transceiver combination, Leigsnering et al. extend the signal model in Eq. (4) as

$$\mathbf{y} = \mathbf{\Phi}^0\mathbf{x} + \mathbf{\Phi}^1\mathbf{x} + \ldots + \mathbf{\Phi}^{R-1}\mathbf{x} \tag{6}$$

Here, $\mathbf{\Phi}^i$ is the dictionary matrix for each propagation path. It is known that there are many other types of multipath returns except the first-order interior wall multipath return. Therefore, the multipath signal model above is an approximate one which will cause model error.

As we all know, FDTD is a numerical technique which can provide a broadband response when simulating electromagnetic wave propagation in a complicated configuration. In this paper, FDTD simulations are exploited to achieve an integrated dictionary matrix $\mathbf{\Phi}^{all}$ for the exact signal model which accounts for all kinds of multipath propagations. Then, the multipath signal model can be written as

$$\mathbf{y} = \mathbf{\Phi}^{all}\mathbf{x} \tag{7}$$

It can be observed that the model of our proposed method is more accurate than the existing signal model. In the signal model, we have added the higher-order interior wall multipath, wall ringing multipath and even target-to-target interaction. Moreover, the complicated computation of time delay when signal travels through or reflects from the wall is avoided.

3. SPARSE RECONSTRUCTION

Within the CS framework, the linear inverse problem can be solved using only a subset of full measurements. Mathematically, a down sampling matrix $\mathbf{\Psi}$ is acted on the full measurements. Particularly, $\mathbf{\Psi}$ is a measurement matrix, each of whose rows has only one nonzero element, which is set to one. This is equal to selecting time samples randomly at each random receiving position.

As such, an under sampled measurement can be acquired

$$\mathbf{z} = \mathbf{\Psi y} = \mathbf{\Psi}(\mathbf{\Phi}^{all})\mathbf{x} = \mathbf{Ax} \tag{8}$$

$\mathbf{A} = \mathbf{\Psi}(\mathbf{\Phi}^{all})$. According to CS theory, provided that the unknown is sparse in a given basis and that the matrix $\mathbf{A}$ fits restricted isometry property (RIP), a high-dimensional signal can be exactly retrieved from a small set of measurements by applying the following optimization problem

$$\min_x \|\mathbf{x}\|_1 \quad \text{subject } \|\mathbf{Ax} - \mathbf{z}\|_{\ l2} \leq \delta \tag{9}$$

The parameter δ depends on the level of required accuracy, on the level of noise of the data and on the model error. The $l1$ minimization method used in this paper is orthogonal matching pursuit (OMP) algorithm. Since the target space for most TWRI applications is sparse, and measurement matrix $\mathbf{\Psi}$ is random to make sure matrix $\mathbf{A}$ fits RIP, TWRI problem can be cast into a sparse reconstruction problem in multipath environment.

4. SIMULATION RESULTS

Numerical examples are presented in this section to demonstrate the capability of the proposed approach. In the first example, a square PEC target is suited in an enclosed room as shown in Fig. 1. The thickness, conductivity and relative permittivity of the walls are 0.1 m, $\sigma = 0.003\,\mathrm{S/m}$, and $\varepsilon_r = 2.75$, respectively. The investigation domain is $D = [-1, 1] \times [0.3, 3.6]\,\mathrm{m}^2$.

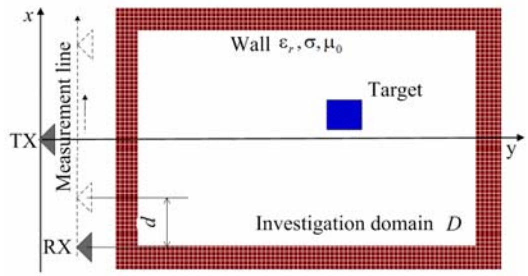

Figure 1. Schematic of through wall geometry.

A bistatic SAR system is assumed for TWRI. Specifically, one transceiver antenna (TX) transmits a UWB short pulse, and the receiver antenna (RX) collects the backscattered fields at each observation point and moves with 0.06 m inner element spacing to synthesize an 2.4 m aperture. Therefore, the element of receiver location is $N = 41$. The scattered fields are simulated and sampled with $M = 1250$ measured data at each antenna location. The investigation domain is discretised to 21×34 pixels with size of $0.1\,\mathrm{m} \times 0.1\,\mathrm{m}$.

Assuming that one target is located at $(0\,\mathrm{m}, 0.9\,\mathrm{m})$, the reconstruction results using original CS and the proposed method with full and limited data are provided in Fig. 2. Original CS method means that only direct propagation path is involved in the dictionary. In the proposed method, the dictionary contains direct and non-direct propagation paths (i.e., multipath propagation) which is constructed using FDTD. Full data measurement means that data are measured at all times and all antenna locations, and limited one means that data are measured at random times and antenna locations. The limited data are about 1% of the full set of data. The true region of the target is indicated with a white square. It is noted that the images are normalized in dB scale with maximum intensity 0 dB.

High-intensity pixels are expected to appear on the left edge of the target because of its impenetrability. As we all known, the image focusing quality is governed by the accuracy of signal model. Aside from the shift of the target position in the range direction, model errors will also lead to widening of point spread functions along the cross-range direction. Therefore, blurred and shifted image will be obtained using original CS even in the full data scenario as depicted in Fig. 2(a). From Fig. 2(c), we can find that the insufficient data will lead to inaccurate result when original CS is used. In other words, $l1$ minimization based method cannot perform well when the multipath is not considered in the signal model for TWRI, while a much more correct and cleaner image is obtained by exploiting multipath signal model in spite of measurement efficiency as shown in Fig. 2(b) and Fig. 2(d). It is noted that some clutters still exist in Fig. 2(b) and Fig. 2(d). It is because there are some clutters left after background subtraction procedure to obtain target returns used for image reconstruction.

In order to evaluate the capability of the proposed method quantitatively, the TCR is introduced [20], which is defined as the ratio between the maximum pixel magnitude value of the target and the average pixel magnitude value in the clutter region

$$\mathrm{TCR} = 20\log_{10}\left(\frac{\max_{(k,l)\in A_t}|I(k,l)|}{\frac{1}{N_c}\sum_{(k,l)\in A_c}|I(k,l)|}\right) \tag{10}$$

Here A_t is the target area, A_c the clutter area, N_c the number of pixels in the clutter area, and $I(k,l)$ the pixel magnitude value at (k,l). Table 1 shows the TCR values for images of one target.

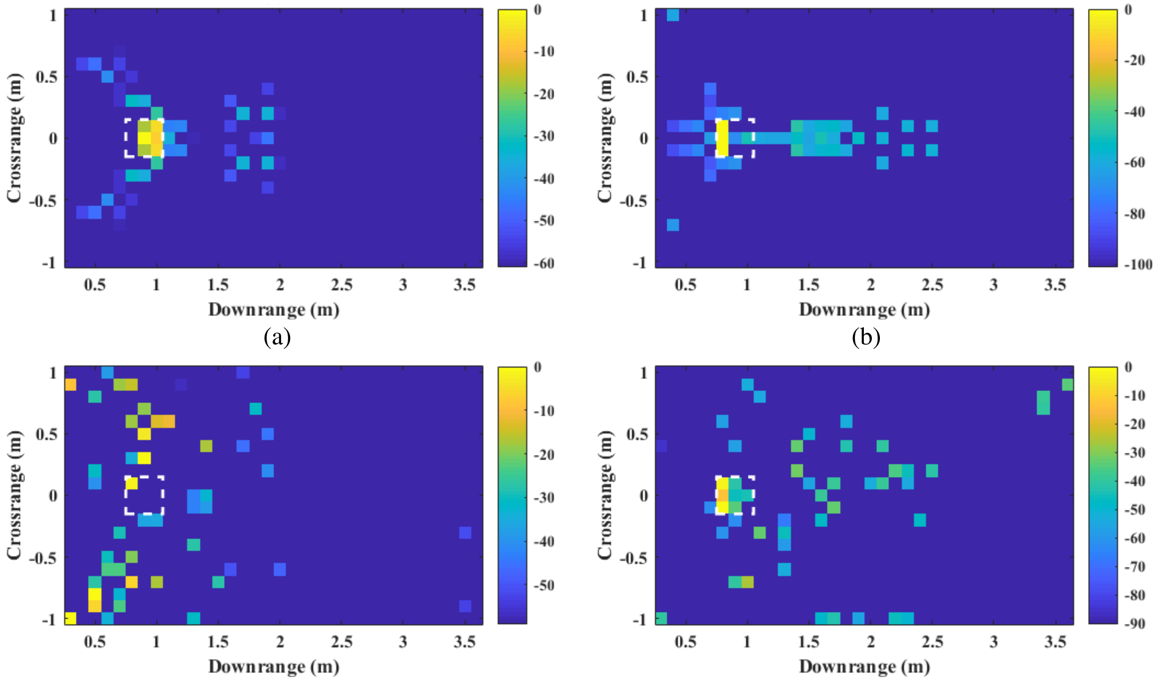

Figure 2. Imaging of a target with location (0 m, 0.9 m) using (a) original CS with full data, (b) the proposed method with full data, (c) original CS with limited data, and (d) the proposed method with limited data.

It is obvious that the TCR is smaller and smaller when the measurement data are less and less. As expected, the TCR for the image of the proposed method is higher than the one for the image of original CS when the data are full or limited. In other words, due to the multipath exploitation, the TCR is much higher which will benefit the detection of the target behind the wall.

Table 1. TCR for images of one target.

	Original CS	Proposed method
With full data	50.4632	59.0832
With limited data	27.5874	51.1647

In order to investigate the robustness of the approach under different noise levels, target returns are corrupted by an additive Gaussian noise with mean value equal to zero and variance fixed according to the desired signal-to-noise ratio (SNR). The TCR as a function of SNR is displayed in Fig. 3. It can be shown that the added noise has almost no effect on TCR when SNR is greater than 60 dB, while TCR decreases rapidly when SNR is smaller than 60 dB.

In the second example, imaging of multiple targets in an enclosed room is presented. The targets under investigation are PEC rectangular and circular cylinders represented by Target 1 and Target 2, respectively. The centred position of Target 1 is located at $(-0\,\mathrm{m}, 2.5\,\mathrm{m})$, and the length of it is 0.3 m. The centred position of Target 2 is located at $(-0.5\,\mathrm{m}, 1\,\mathrm{m})$, and the radius of it is 0.15 m. Fig. 4 shows the image results using sparse reconstruction and the proposed method with full and limited data. The same as the first example, the limited measured data are about 1% of full data. Moreover, TCR values for images of multiple targets are listed in Table 2.

From Figs. 4(a), (c), we find that lacking of multipath exploitation will defocus target image, displace from its true position, and possibly produce false target even when the full data are used.

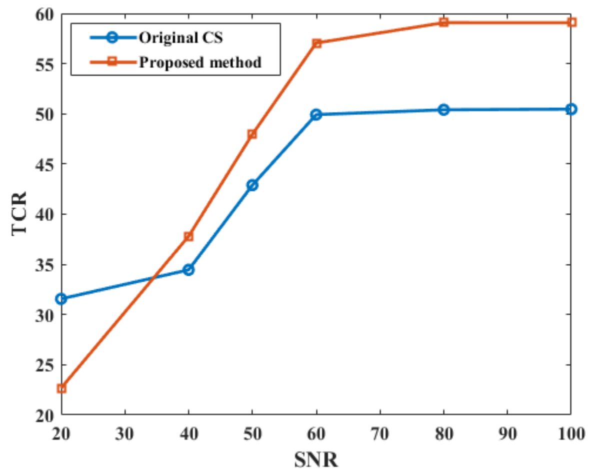

Figure 3. TCR for images of one target as a function of SNR when original CS and the proposed method are used.

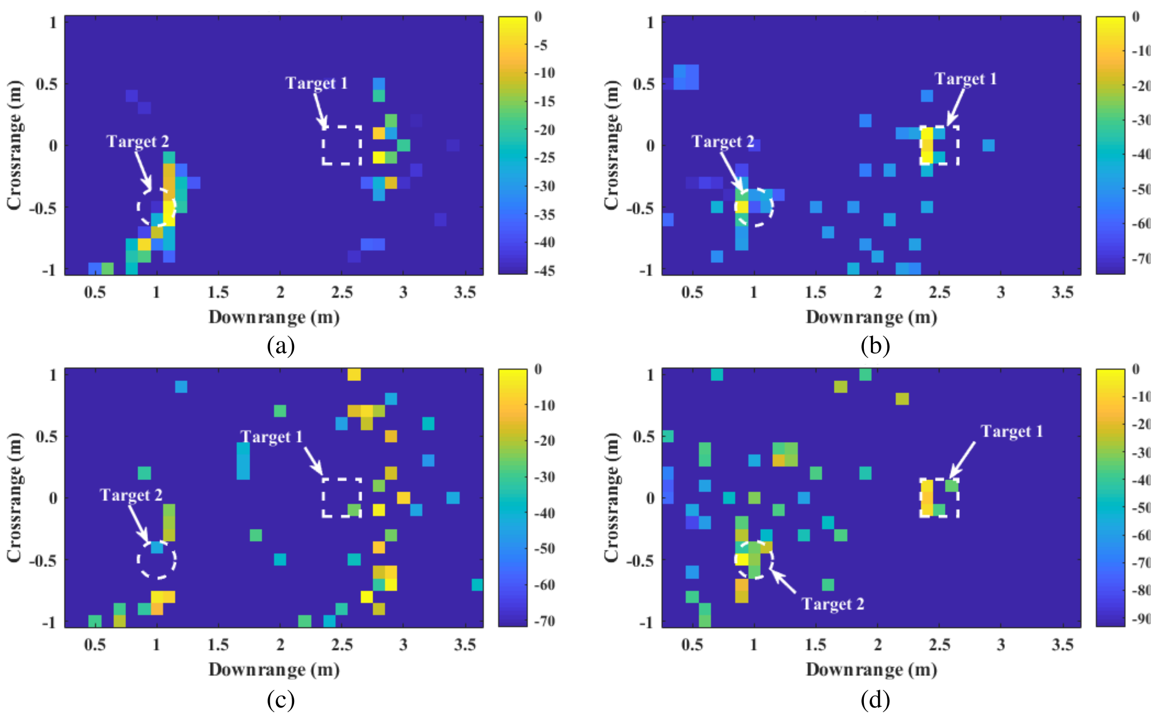

Figure 4. Imaging of two targets using (a) original CS with full data, (b) proposed method with full data, (c) original CS with limited data, and (d) proposed method with limited data.

Figs. 4(b) and (d) show that by exploiting the multipath signal model, reconstruction results based on the proposed method are superior to original CS method even when the measurement data are not sufficient. The same as Figs. 2(b) and (d), there are some clutters due to imperfect background subtraction.

Since the multipath propagation is incorporated into the exact signal model calculated by FDTD, TCR values listed in Table 2 demonstrate that the reconstruction results based on the proposed method are less cluttered and have lower side-lobe levels than the one reconstructed by original CS method regardless of measurement data.

Table 2. TCR for images of multiple targets.

	Original CS	Proposed method
With full data	39.1909	55.7049
With limited data	36.7906	46.1518

Also, an additive Gaussian noise with mean value equal to zero and variance fixed according to the desired signal-to-noise ratio (SNR) is added to the target return. The TCR as a function of SNR in the second experiment is displayed in Fig. 5. Generally speaking, the curves, showing the TCR versus SNR, are similar to the ones in Fig. 3.

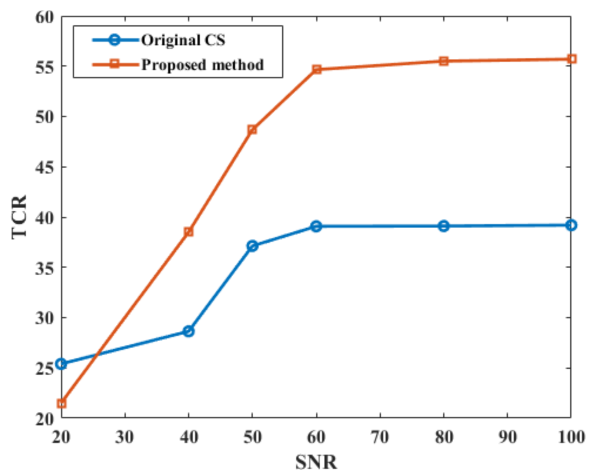

Figure 5. TCR for images of multiple targets as a function of SNR when original CS and the proposed method are used.

5. CONCLUSIONS

Ghosts caused by multipath have been widely researched in TWRI. In this paper, we present an approach which combines sparse image reconstruction and FDTD technique for multipath ghost suppression. Under the framework of sparse reconstruction, we modelled various multipath returns in the over-complete dictionary which relates the measurement signal and the image space using FDTD simulation. Simulated results show that a much more correct and cleaner image is obtained by exploiting multipath signal model in spite of measurement efficiency, and the proposed approach can also suppress ghost when far few measurement data are used.

ACKNOWLEDGMENT

We want to thank the helpful comments and suggestions from the anonymous reviewers. This work was supported by the National Natural Science Foundation of China (Grant No. 61601245 61601242), and State Key Laboratory of Millimeter Waves Open Project, Southeast University (Grant No. K201724), China Postdoctoral Science Foundation Funded Project (Grant No. 2016M601693) and Nanjing University of Posts and Telecommunications Foundation, China (Grant No. NY214047).

REFERENCES

1. Amin, M. and K. Sarabandi, "Special issue on remote sensing of building interior," *IEEE Geoscience & Remote Sensing Letters*, Vol. 5, 118–118, 2008.

2. Amin, M. G., *Through-the-Wall Radar Imaging*, CRC Press, 2010.
3. Yektakhah, B. and K. Sarabandi, "All-directions through-the-wall radar imaging using a small number of moving transceivers," *IEEE Transactions on Geoscience & Remote Sensing*, Vol. 54, 6415–6428, 2016.
4. Herman, M. A. and T. Strohmer, "High-resolution radar via compressed sensing," *IEEE Transactions on Signal Processing*, Vol. 57, 2275–2284, 2009.
5. Donoho, D. L., "Compressed sensing," *IEEE Transactions on Information Theory*, Vol. 52, 1289–1306, Apr. 2006.
6. Candes, E. J., J. Romberg, and T. Tao, "Robust uncertainty principles: Exact signal reconstruction from highly incomplete frequency information," *IEEE Transactions on Information Theory*, Vol. 52, 489–509, 2004.
7. Huang, Q., L. Qu, B. Wu, and G. Fang, "UWB through-wall imaging based on compressive sensing," *IEEE Transactions on Geoscience & Remote Sensing*, Vol. 48, 1408–1415, 2010.
8. Wu, Q., Y. D. Zhang, F. Ahmad, and M. G. Amin, "Compressive-sensing-based high-resolution polarimetric through-the-wall radar imaging exploiting target characteristics," *IEEE Antennas & Wireless Propagation Letters*, Vol. 14, 1043–1047, 2015.
9. Zhang, W. and A. Hoorfar, "A generalized approach for SAR and MIMO radar imaging of building interior targets with compressive sensing," *IEEE Antennas & Wireless Propagation Letters*, Vol. 14, 1052–1055, 2015.
10. Wang, X., G. Li, Y. Liu, and M. G. Amin, "Two-level block matching pursuit for polarimetric through-wall radar imaging," *IEEE Transactions on Geoscience & Remote Sensing*, Vol. 99, 1–13, 2018.
11. Burkholder, R. J., "Electromagnetic models for exploiting multi-path propagation in through-wall radar imaging," *International Conference on Electromagnetics in Advanced Applications*, 572–575, 2009.
12. Gennarelli, G. and F. Soldovieri, "Multipath ghosts in radar imaging: Physical insight and mitigation strategies," *IEEE Journal of Selected Topics in Applied Earth Observations & Remote Sensing*, Vol. 8, 1078–1086, 2015.
13. Liu, J., L. Kong, X. Yang, and Q. H. Liu, "First-order multipath ghosts' characteristics and suppression in MIMO through-wall imaging," *IEEE Geoscience & Remote Sensing Letters*, Vol. 13, 1315–1319, 2016.
14. Setlur, P., M. Amin, and F. Ahmad, "Multipath model and exploitation in through-the-wall and urban radar sensing," *IEEE Transactions on Geoscience & Remote Sensing*, Vol. 49, 4021–4034, 2011.
15. Setlur, P., G. Alli, and L. Nuzzo, "Multipath exploitation in through-wall radar imaging via point spread functions," *IEEE Transactions on Image Processing*, Vol. 22, 4571, 2013.
16. Leigsnering, M., M. Amin, F. Ahmad, and A. M. Zoubir, "Multipath exploitation and suppression for SAR imaging of building interiors: An overview of recent advances," *IEEE Signal Processing Magazine*, Vol. 31, 110–119, 2014.
17. Leigsnering, M., F. Ahmad, M. Amin, and A. Zoubir, "Multipath exploitation in through-the-wall radar imaging using sparse reconstruction," *IEEE Transactions on Aerospace & Electronic Systems*, Vol. 50, 920–939, 2014.
18. Leigsnering, M., F. Ahmad, M. G. Amin, and A. M. Zoubir, "Parametric dictionary learning for sparsity-based TWRI in multipath environments," *IEEE Transactions on Aerospace & Electronic Systems*, Vol. 52, 532–547, 2016.
19. Dogaru, T. and C. Le, "SAR images of rooms and buildings based on FDTD computer models," *IEEE Transactions on Geoscience & Remote Sensing*, Vol. 47, 1388–1401, 2009.
20. Lagunas, E., M. G. Amin, F. Ahmad, and M. Najar, "Joint wall mitigation and compressive sensing for indoor image reconstruction," *IEEE Transactions on Geoscience and Remote Sensing*, Vol. 51, 891–906, Feb. 2013.